INSTITUTE OF PHYSICS PUBLISHING JOURNAL OF PHYSICS B: ATOMIC, MOLECULAR AND OPTICAL PHYSICS

J. Phys. B: At. Mol. Opt. Phys. **36** (2003) 3707–3719 PII: S0953-4075(03)60643-7

# A pseudo-state sensitivity study on hydrogenic ions

**C P Ballance**[1], **N R Badnell**[2] **and E S Smyth**[3]

[1] Department of Physics, Rollins College, Florida, FL 32789, USA
[2] Department of Physics, University of Strathclyde, Glasgow G4 0NG, UK
[3] NAG Ltd, Wilkinson House, Jordan Hill Road, Oxford O2 8DR, UK

Received 6 March 2003, in final form 4 July 2003
Published 27 August 2003
Online at stacks.iop.org/JPhysB/36/3707

**Abstract**

An electron-impact excitation study of light hydrogenic ions has been carried out to quantify the effects of coupling to high bound/continuum states utilizing the *R*-matrix with pseudo-states method. As the ionization stage increases, the neglect of loss of flux into high-lying excitation/ionization channels impacts less upon excitation between the bound terms explicitly included within our close coupling expansion.

$C^{5+}$ is used as our benchmark study. The differences in Maxwell averaged collision strengths between a standard *R*-matrix calculation and those of a similar pseudo-state model across a range of temperatures shall be our criteria for judging differences.

We carried out calculations for $He^{+}$, $Li^{2+}$, $Be^{3+}$, $B^{4+}$, $C^{5+}$, $O^{7+}$ and $Ne^{9+}$ so as to provide excitation data amongst terms up to $n = 5$. Pseudo-state calculations were carried out for the first five ions, following a similar model to earlier neutral hydrogen work, whilst non-pseudo-state calculations sufficed for the remaining two ions. The results of these seven calculations will enhance existing excitation data sets for use in the modelling of controlled nuclear fusion plasma experiments.

(Some figures in this article are in colour only in the electronic version)

## 1. Introduction

Bray and Stelbovics (1993) illustrated the importance of continuum coupling in the electron-impact excitation of neutral hydrogen. We have now carried out a range of calculations on hydrogenic ions so as to determine these effects as a function of nuclear charge $Z$ using the RMPS (*R*-matrix with pseudo-states) method. The ions under study range from $He^{+}$ to $Ne^{9+}$. There have been many piecewise studies of hydrogenic systems but, again, there is a demand for *complete* sets of effective collision strengths for spectroscopic modelling and plasma diagnostics (Summers 1999). This will impact upon collisional radiative modelling that takes charge transfer into account. Highly ionized carbon and oxygen incident on either

  

hydrogen or helium tend to capture into shells with principal quantum numbers $n = 4$ and 5. (Phaneuf *et al* 1987). Furthermore, visible spectroscopy utilizes lines that originate from $n = 7$ or 8. Hence, it is also important to be able to extrapolate collision data reliably from $n = 5$, say.

In the case of $He^+$ we shall refer to the work Kisielius *et al* (1996) who carried out a 25 level Dirac $R$-matrix calculation (Norrington and Grant 1987). They provide low-temperature effective collisions strengths between the first 16 of their 25 levels. We are able to compare with their results after averaging over the fine structure levels. For higher energy comparisons, we have the convergent close coupling (CCC) results of Bray[4] with which to compare.

There have been very few resonance-resolved electron excitation studies carried out on $Li^{2+}$, and the majority of those published in the 1970s and 1980s have been classified by Pradhan and Gallagher (1992) in their evaluated compilation as being 'average to poor'. The few low-energy points provided by Morgan (1980) are the only exception. She also provides results for $Ne^{9+}$ at the same $Z$-scaled energies.

Berrington and Clarke (1993) provided a compendium of fitted data for electron-impact excitation and ionization of $Be^{q+}$ and $B^{q+}$ in which non-pseudo-state $R$-matrix calculations were used in conjunction with distorted waves. Badnell and Gorczyca (1997) improved upon these models by including a substantial number of pseudo-states and highlighted the effects of continuum coupling on $Be^{3+}$ and $B^{4+}$ as well as lighter ions, but their results were not complete enough to provide effective collision strengths. Their preliminary study of iso-electronic trends for continuum coupling effects focused on 1s–2s, 1s–5s and 4s–5s transitions. We are interested in the effects along monopole (1s, 2s $\rightarrow$ $n$s) and dipole (1s, 2s $\rightarrow$ $n$p) transition sequences, and also obtain results for quadrupole etc transitions. Be and B are two key materials under study for utilization in the next generation of magnetic fusion reactors and accurate data for these ions is currently required.

The first comprehensive study of $C^{5+}$ within an $R$-matrix framework was carried out by Aggarwal and Kingston (1991a). They appreciated that their model lacked pseudo-states to account for loss of flux into various excitation and ionization channels, as implemented in the work of Abu-Salbi and Callaway (1981). They concluded that the inclusion of pseudo-states was beyond their computational abilities at that time; however, we are now in a position to include them.

The results for two further species, $O^{7+}$ and $Ne^{9+}$, shall be presented, of which $O^{7+}$ was also considered by Abu-Salbi and Callaway (1981). Their comparisons with the results of the distorted wave approach of Mann (unpublished) showed a decrease in collision strengths of approximately 20% for the 1s–2s case. Estimated differences of only 6% in thermally averaged collision strengths due to resonant enhancement may seem minimal, but their effective collision strengths start at 100 eV.

Highly ionized ions may not experience the same degree of continuum coupling but, due to the increased height of Rydberg series, they require a sufficiently dense energy grid to resolve resonances fully. At lower temperatures, effective collision strengths, especially weak transitions, can be influenced strongly by resonance contributions. It should be noted that, apart from previous $R$-matrix studies, the resonances attached to the $n = 4$–6 terms are seldom accounted for.

It has been proposed that the next generation of soft x-ray satellites, observing high resolution spectra, will use highly ionized oxygen lines. Constellation-X,[5] a satellite capable of soft x-ray observations, will investigate the inter-galactic medium using the resonance lines of O VII and O VIII at 574 and 654 eV, respectively.

[4] http://atom.murdoch.edu.au/CCC-WWW/
[5] http://constellation.gsfc.nasa.gov/docs/science/igm2.html

The remainder of the paper shall be structured as follows. The following section shall give an overview of the target states included in each of the $R$-matrix calculations. In the cases where a pseudo-orbital basis is implemented we shall give its extent and justify its use. The subsequent section shall take each element in turn and compare with other studies in the literature with an emphasis on those that have taken the effects of continuum coupling and/or resonances into account. In the conclusions we shall highlight the points of interest from this isoelectronic sequence.

## 2. Calculations

We have used AUTOSTRUCTURE (Badnell 1997) to generate the orbitals used in our close coupling expansion. The $He^+$ and $Li^{2+}$ calculations included all 15 physical $LS$ terms up to $n = 5$, supplemented by 24 pseudo-states to account for high bound/continuum coupling. These Laguerre pseudo-orbitals ranging from $\bar{n} = 6$–9 and $\bar{l} = 0$–5 span the energy range from just below the ionization threshold to approximately twice this value. This set of non-orthogonal Laguerre orbitals take the form

$$P_{nl}(r) = N_{n\ell}(\lambda_\ell Zr)^{l+1}\mathrm{e}^{-\lambda_\ell Zr/2}L_{n+l}^{2\ell+1}(\lambda_\ell Zr). \tag{1}$$

In this equation, $Z = z + 1$, where $z$ is the residual charge on the ion, $L_{n+l}^{2\ell+1}(\lambda_\ell Zr)$ represents the Laguerre polynomial and $N_{n\ell}$ is a normalization constant. These Laguerre orbitals were then orthogonalized to the spectroscopic orbitals and to each other. For every system the $\lambda_\ell$ screening parameters were set equal to 1.

This choice of pseudo-orbitals was implemented as a result of our experience with neutral hydrogen (Anderson *et al* 2000). Various tests were carried varying $\bar{n}$ and $\bar{l}$ so as to ensure collision strength convergence for selected partial waves. We ensured that one layer of $n = 6$ terms remained below the ionization limit to account for high-lying bound terms omitted from our close coupling expansion. AUTOSTRUCTURE is also used to calculate the Bethe and Born limits required to interpolate collision strengths to temperatures unattainable from the final calculated $R$-matrix values. As we are pursuing $LS$-resolved hydrogenic ions, every transition should have a high energy limit point. We have not presented target eigenenergies, though in the hydrogenic case, they are given by the simple formula

$$E(nl) = (1 - 1/n^2)Z^2 \tag{2}$$

where $E(nl)$ is the energy in rydbergs relative to the ground state, $n$ is the principal quantum number and $Z$ the nuclear charge of the ion.

More emphasis was given to $C^{5+}$, wherein we carried out two separate calculations. Firstly, a non-pseudo-state model which included the 21 $LS$ terms up to $n = 6$ and a second model which included spectroscopic terms up to $n = 5$ but with six layers of pseudo-states. These pseudo-orbitals ranged from $\bar{n} = 6$–11 and $\bar{l} = 0, 5$. The reason for the seeming mismatch between the spectroscopic terms included in both models is because the lowest layer of pseudo-states below the ionization threshold tends to take on the characteristics of bound states approximately equivalent to the extra layer of physical $n = 6$ terms. We are trying to quantify in the case of hydrogenic targets a cut-off point where electron excitation amongst bound terms does not compete with ionization.

In the case of $O^{7+}$ and the $Ne^{9+}$, we did not include any pseudo-orbitals and included physical terms up to $n = 5$ and 6, respectively. From an $R$-matrix perspective, an $n = 6$ model is more computationally demanding due to the increasingly diffuse 6s orbital, which is theoretically required to be fully encompassed within the $R$-matrix hypersphere.

The $R$-matrix codes of Berrington *et al* (1995), as modified by Badnell and Gorczyca (1997) to handle a large pseudo-state expansion rigorously, were used to span the incident

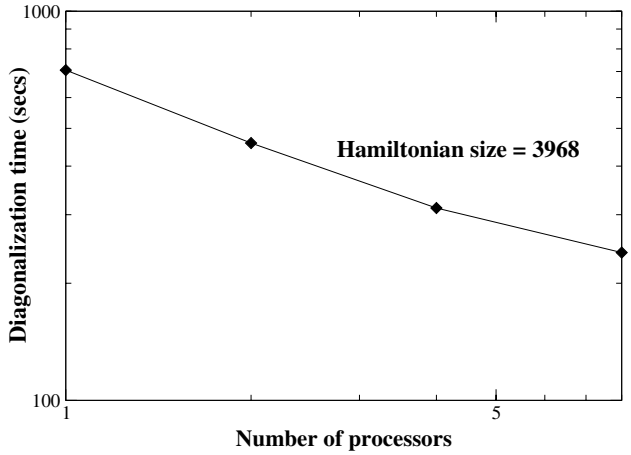


**Figure 1.** Execution time for DSYEVR on a 400 MHz SGI origin 3000 using the SCSL math library. For comparison, HSLDR takes 2884 s for the same problem.

**Table 1.** The different scattering models used for hydrogenic ions.

| | $He^{+}$ | $Li^{2+}$ | $Be^{3+}$ | $B^{4+}$ | $C^{5+}$ | $O^{7+}$ | $Ne^{9+}$ |
|---|---|---|---|---|---|---|---|
| Spectroscopic terms | 15 | 15 | 15 | 15 | 15 | 15 | 21 |
| Pseudo-states terms | 24 | 24 | 24 | 24 | 36 | — | — |
| $\bar{n}$ | 6–9 | 6–9 | 6–9 | 6–9 | 6–11 | — | — |
| $\bar{l}$ | 0–5 | 0–5 | 0–5 | 0–5 | 0–5 | — | — |
| Continuum basis size | 49 | 49 | 49 | 49 | 60 | 70 | 71 |

electron energy range to at least twice the ionization threshold. In general, as the hydrogenic species become more highly ionized, the radial extent of the bound orbitals tends to contract. Consequently, the size of the continuum basis that is orthogonalized to these bound and/or pseudo-orbitals varies from species to species. Table 1 shows the orbital description of every case as well as the size of the continuum basis. In the case of $Ne^{9+}$, we have taken advantage of the decrease in continuum basis size and included an extra layer of physical $n = 6$ terms.

Until recently, the biggest computational 'bottleneck' in an $R$-matrix calculation (compounded by the use of increasing numbers of pseudo-states) tended to be the diagonalization of an inner-region Hamiltonian. The resulting surface amplitudes and $R$-matrix poles are required to link the many-bodied calculation inside the $R$-matrix hypersphere with a simpler two-bodied one beyond its radius.

We have replaced the STG3 diagonalization routine HSLDR (Householder) by a call to the LAPACK[6] routine DSYEVR. DSYEVR requires more memory than HSLDR, but runs much more efficiently by better exploiting the cache memory on modern microprocessor-based systems. It also allows the user to transparently access parallelism on multiprocessor systems, where the LAPACK library (or the underlying BLAS routines) have been parallelized. This can quickly reduce the computational time by an order of magnitude, as demonstrated in figure 1. A symmetric matrix of rank 3968 corresponding to the $^{1}G^{e}$ partial wave of $Ne^{9+}$ is the given example.

[6] http://www.netlib.org/lapack/

We expect that the continuum coupling should be strongly evident in the lower charge species, but this influence should be restricted to symmetries with low-$L$ values. Therefore, we have used a modified version of the non-exchange code (Burke *et al* 1992) including only the spectroscopic terms to account for partial waves between $L = 13$–$60$. Top-up procedures were implemented beyond this point but only had an effect in the case of near degenerate dipole transitions amongst high-lying terms. The non-exchange code takes advantage of the same LAPACK diagonalization routine used in the exchange code, but also calculates the eigenvectors and eigenvalues of a diminishing Hamiltonian matrix as we proceed to higher partial waves due to a progressive reduction in the size of the continuum orbital basis required. In the case of the two most highly ionized species, we only needed to use the exchange code with partial waves generated up to $L = 20$ before the top-up procedures were applied.

The solution in the outer region was performed using a modified version of the unpublished code STGF. As the height of a Rydberg series increases with ionic charge, the question of resonance resolution becomes pertinent as we progress to hydrogen-like oxygen and neon. The energy mesh used for each species shall be discussed in the following subsections.

In general, the greatest effort has gone into resolving the resonances below the ionization threshold, with a coarse mesh beyond to give a smooth shape to the asymptotic form of the collision strength beyond that. However, we have removed transitions within the same complex from the final set of results because of the $LS$ degeneracy in the target terms.

Maxwell averaged effective collision strengths derived from our data can be used in plasma modelling. However, determination of effective collision strengths over a wide range of temperatures requires that our calculated collision strengths be extended to higher energies. To explicitly extend the $R$-matrix calculation to high enough energies to ensure closure within our effective collision strength integrals would eventually become computationally intractable. Hence, we rely on the work of Burgess and Tully (1992) and Burgess *et al* (1997) in which explicitly calculated $R$-matrix collision strengths can be interpolated to high-energy Bethe/Born limits on a reduced energy scale. Recently, Badnell and Thomas (see Whiteford *et al* 2001) implemented and extended these expressions within AUTOSTRUCTURE (Badnell 1997) for all multipoles.

The full set of results for energy levels, dipole radiative rates and effective collision strengths over a range of temperature (including Born limits), tabulated in the ADAS *adf04* format (Summers 1994, 1999), is available via the WWW at http://www-cfadc.phy.ornl.gov/data_and_codes/.[7]

## 3. Results

### *3.1. $He^+$*

The Dirac $R$-matrix investigation of Kisielius *et al* (1996) presents effective collision strengths amongst all levels up to $n = 4$. In general, the agreement is reasonable considering that between $\log(T\ (\mathrm{K})) = 3.2$–$4.3$ the effective collision strength will be exceedingly sensitive to resonance resolution and threshold positions. They used 'more than 5500' points in the dense Rydberg structure below the ionization threshold compared with the 12 000 points used in the present study. Their model did not employ pseudo-states to represent high bound/continuum coupling but at these low temperatures such effects are expected to be minimal. In table 2 we have averaged their level resolved results from their table 4 to compare with our $LS$ effective

[7] One of the authors (CPB) will be glad to provide all the effective collision strengths in electronic form to the interested reader (ballance@vanadium.rollins.edu).

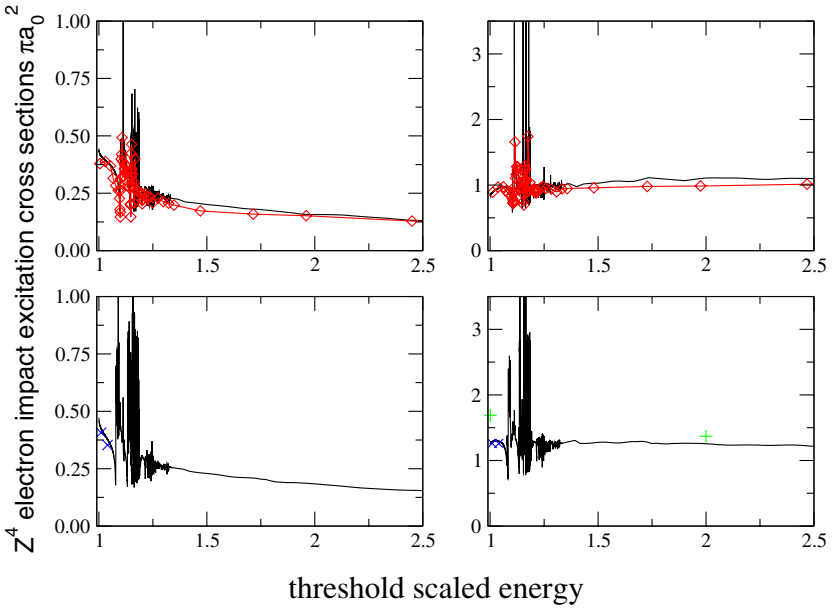


**Figure 2.** $Z^4$-scaled electron-impact excitation cross sections, in $(\pi a_0^2)$ for the 1s–2s (left column) and 1s–2p (right column) transitions. $He^+$ corresponds to the top graphs; with $Li^{2+}$ below. Diamonds, CCC results; diagonal crosses, Morgan (1980), vertical crosses, Mitra and Sil (1978) solid curve, present work.

**Table 2.** *LS*-resolved effective collision strengths from the ground state of $He^+$.

| | $\log_{10}(T)$ | | | | |
|---|---|---|---|---|---|
| Transition | 3.2 | 3.5 | 4.0 | 4.3 | Largest difference (%) |
| 1s–2s | 1.76(−1)[a] | 1.73(−1) | 1.67(−1) | 1.62(−1) | 7.78 |
| | **1.59(−1)**[b] | **1.58(−1)** | **1.54(−1)** | **1.51(−1)** | |
| 1s–2p | 3.33(−1) | 3.40(−1) | 3.58(−1) | 3.78(−1) | 4.42 |
| | **3.19(−1)** | **3.26(−1)** | **3.45(−1)** | **3.65(−1)** | |
| 1s–3s | 5.04(−2) | 4.74(−2) | 4.67(−1) | 4.55(−2) | 30.6 |
| | **3.39(−2)** | **3.14(−2)** | **3.71(−2)** | **3.75(−2)** | |
| 1s–3p | 6.95(−2) | 6.74(−2) | 7.26(−2) | 7.69(−2) | 28.9 |
| | **4.94(−2)** | **5.09(−2)** | **6.01(−2)** | **6.55(−2)** | |
| 1s–3d | 5.57(−2) | 5.14(−2) | 4.70(−2) | 4.40(−2) | 17.7 |
| | **4.58(−2)** | **4.34(−2)** | **4.14(−2)** | **3.95(−2)** | |

[a] Kisielius *et al* (1996).
[b] Present work.

collision strengths. Their results for the 1s–3p transition behave erratically at low temperatures, but agreement improves with increasing temperature.

Aggarwal *et al* (1992) adopted a hybrid approach by meshing together the results of an earlier non-pseudo-state $n = 5$ $R$-matrix calculation with those of the $n = 3$ pseudo-state calculation by Unnikrishnan *et al* (1991), above the ionization limit. They discuss a 25% drop in the collision strength background for the 1s–2s transition, which seems to be in accord with our own work. They also reported a slight disagreement for the 1s–3d transition, namely that

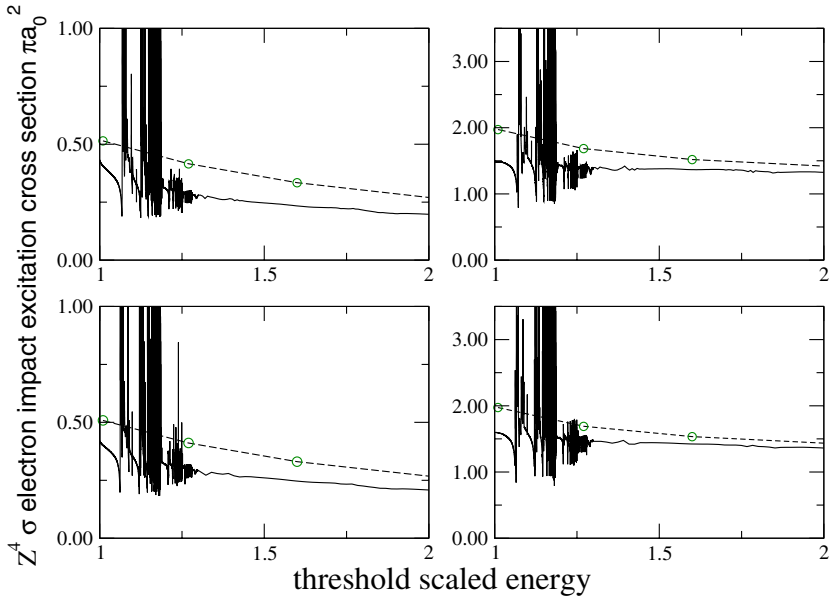


**Figure 3.** $Z^4$-scaled electron-impact excitation cross sections, in ($\pi a_0^2$), for the 1s–2s (left column) and 1s–2p (right column) transitions. $Be^{3+}$ corresponds to the top graphs, with $B^{4+}$ below. Dashed curve with circles, Berrington and Clarke (1993); solid curve, present work.

the effective collision strength actually increases with pseudo-state inclusion. In our model we did not find this to be the case, our results being below their earlier non-pseudo-state results. The results from the CCC method, which takes into account the loss of flux into the ionizing channels, also exhibits good agreement with our results from the ground state to the $n = 2$ terms, as shown in figure 2. However, the present calculation delineates the large Rydberg structure below the $n = 3$ terms better, and reveals those series attached to the $n = 4$ and 5 thresholds. Our model employs over 10 000 energy points in the 1 Ryd region between the first excited term and the ionization threshold, so we have great confidence that any prominent Rydberg structure has been resolved. Figures 2–4, by $Z^4$ scaling of the cross section to the $n = 2$ terms, put each species in the context of the isoelectronic trend. Not surprisingly, the singly ionized case shows the greatest degree of continuum coupling. At low-scattering energies, the 1s–2p $Z^4$ cross section has a value below 1.0, yet $Li^+$, the next element in the isoelectronic sequence, has a value approximately one third higher. The 1s–2s transition appears to be less sensitive to the presence of pseudo-states along the isonuclear sequence. This is shown by the left columns of figures 2–4 having very similar values across a range of incident electron energies.

### *3.2. $Li^{2+}$*

There has been a concerted effort amongst the authors to provide all the isoelectronic electron-impact excitation data required of lithium for spectroscopic modelling. The helium-like lithium case (Ballance *et al* 2002) is probably one of the most extensive pseudo-state expansions in the literature to date with inner-region Hamiltonian matrices close to 17 000 in rank, although recent beryllium-like targets, for example $C^{2+}$ (Mitnik *et al* 2003), have two such sequences, $1s^2 2s nl$ and $1s^2 2p n'l'$. Hydrogen-like lithium will contribute to the data required for plasma

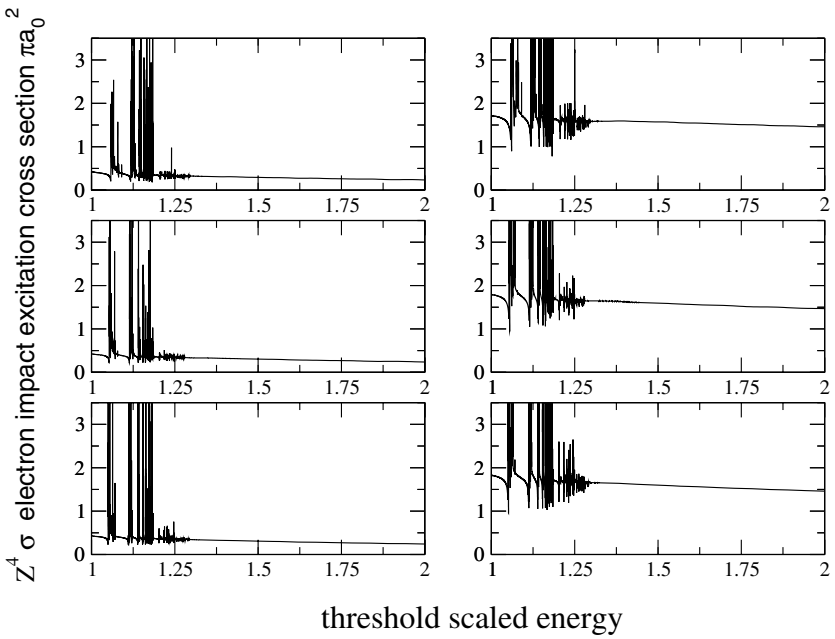


**Figure 4.** $Z^4$-scaled electron-impact excitation cross sections, in $(\pi a_0^2)$, for the 1s–2s (left column) and 1s–2p (right column) transitions. The results for $C^{5+}$, $O^{7+}$ and $Ne^{9+}$ are given in descending order.

transport codes used in DIII-D fusion experiments (San Diego). These codes will analyse the ionization and transportation of lithium introduced into the tokamak via a probe. Electron-impact scattering calculations which take into account continuum coupling have been scarce for $Li^{2+}$. As the review paper of Pradhan and Gallagher (1992) suggests, the highly rated calculations tended to provide only a couple of excitations from the ground state and for a few energy points. These provide an qualitative check of the background collision strength, but not the comprehensive set of transitions that we provide.

We compare our results with the low-energy results of Morgan (1980) in figure 2 and the agreement for the few energy points available is good. The CBO (Coulomb–Born–Oppenheimer) values of Mitra and Sil (1978) are about a third higher just above threshold, but give reasonable answers at twice this value.

The distorted wave results of Clark (1990) show differences bordering on a factor of 2 at low energies. This is illustrated in figure 7 in which the summed excitation from the $n = 3$ to 4 terms of our RMPS calculation only gradually converge with the distorted wave results at nearly twice the ionization limit.

### *3.3. $Be^{3+}$ and $B^{4+}$*

For these two systems we compare with the work of Berrington and Clarke (1993), as illustrated in figure 3. Even when the target is ionized three to four times the difference between the distorted wave and the present RMPS results is roughly 25% close to the 2s and 2p thresholds. Yet at the threshold energy of 2.0 Ryd, both sets of results between all models are consistent, with the $B^{4+}$ case having marginally better agreement. At higher charge states, there is an expansion of the low-energy resonance region between the first threshold and the ionization

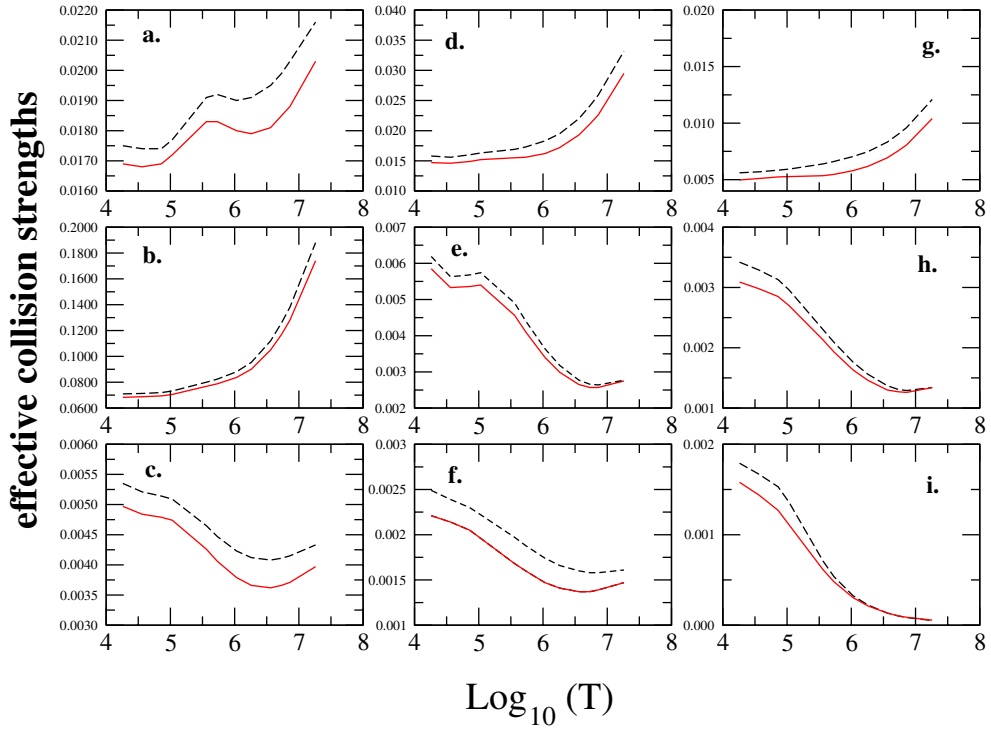


**Figure 5.** Effective collision strength comparisons between pseudo-state and non-pseudo-state models in $C^{5+}$. Excitations from the ground state to all $n \leqslant 4$ terms are given in consecutive order in graphs (a)–(i). Dashed curve, non-pseudo-state; solid curve, pseudo-state.

limit. For both ions, a fine energy grid of ≈0.000 02 Ryd was used from between the first excited threshold up to just beyond the last. Over 20 000 energy points were used in the case of $Be^{3+}$ and over 17 000 for $B^{4+}$ to ensure the same degree of resonance delineation accorded to previous ions; with a coarse energy grid beyond that. Studies are underway to examine the effects of including threshold scaled energies interwoven among the linear energy grid to assess their impact on low-temperature effective collision strengths.

### *3.4. $C^{5+}$*

When a hydrogenic system is ionized five times we would expect coupling to the continuum to become negligible. However, we thought that it would beneficial to quantify these effects and, if they can be neglected, it opens the opportunity for more physical bound orbitals to be included in our close coupling expansion. Particular attention will be paid to strong dipole transitions in which the final state is positioned close to the ionization limit. The pseudo-state calculation is probably the largest attempted for a hydrogenic $R$-matrix case, in which the 15 spectroscopic terms are used in conjunction with 36 pseudo-orbitals. We ensured that the $\bar{n}$ terms provided a set of doublets ranging from $\bar{l} = 0$–5 below the ionization limit were mirrored by a set of $\bar{n} = 6$ terms just above. This prevents any major oscillations in the collision strength in this energy region which can influence low-temperature effective collision strengths. These six layers of pseudo-states are comparable to our recent $Li^{+}$ study (Ballance *et al* 2002) in which we found that coupling to the continuum and high bound states persisted well below

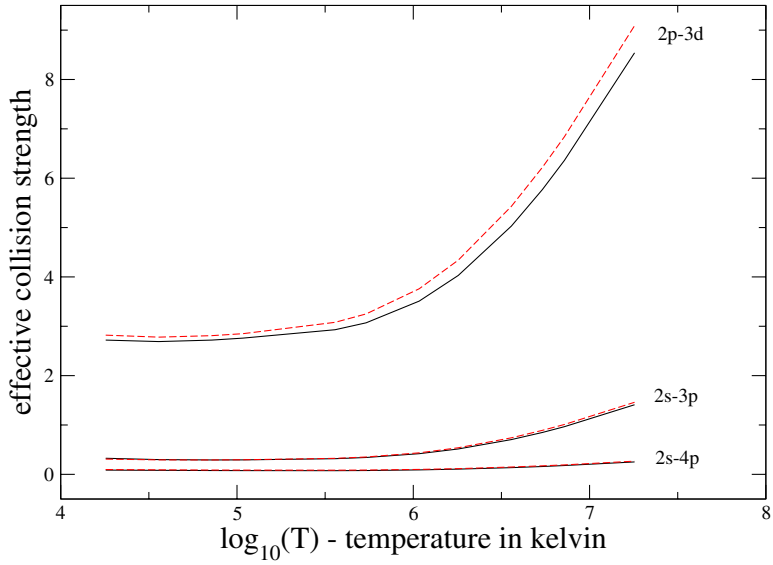


**Figure 6.** Dipole-allowed effective collision strengths from the $n = 2$ terms of $C^{5+}$. Dashed curve, non-pseudo-state; solid curve, pseudo-state.

the ionization limit. The pseudo-states are clustered around the ionization limit, with an even distribution up to 50 Ryd, before the final ten terms are unevenly and sparsely distributed over the next 150 Ryd. Figure 5 shows the comparison between the results of the two calculations. This matrix of effective collision strengths represents all transitions from the 1s ground state to terms with $n \leqslant 4$. The strong dipoles (1s–$n$p) labelled (b), (d) and (g) respectively differ at most by 17%, and generally have agreement to better than 10%.

The monopole transitions (a) and (c) are particularly sensitive to the large Rydberg resonances attached to the $n = 3$ and 4 terms. This manifests itself as an undulation in the effective collision strength in the $\log(T\ (\mathrm{K})) = 5$–6 range. Furthermore, the pseudo-states lower the background collision strength by only 2–3%.

The quadrupole transitions (e) and (h) also exhibit, to a lesser degree, a 'bump' at $\log(T\ (\mathrm{K})) = 5$ in their Maxwell averaged collision strengths, though agreement by $\log(T\ (\mathrm{K})) = 7$ is excellent. In general, transitions involving large energy separations are the most affected by continuum coupling. This reduction in the collision strength is further accentuated by the proximity of the final term to the ionization threshold. Strong dipole excitations from the 2s, 2p terms as illustrated in figure 6 maintain better agreement across a range of temperatures than those from the ground state.

Aggarwal and Kingston (1991a) have also provided results from an $n = 5$ $R$-matrix model without pseudo-states, but we would disagree with their presentation of transitions within terms of the same principal quantum number. As illustrated in table 1 of their paper, the eigenenergies of their target terms having the same principal quantum number are absolutely degenerate, and would result in infinite collision strengths if Burgess top-up procedures were used. They quote using a mesh of the 'order of 0.001' in resonance regions and a coarser mesh beyond that resulting in a total of 1767 energy points. We have used a mesh of 7000 points in the case of the pseudo-state calculation and over 12 000 in the non-pseudo-state case, with the emphasis on resolving resonances in the region below the $n = 5$ terms.

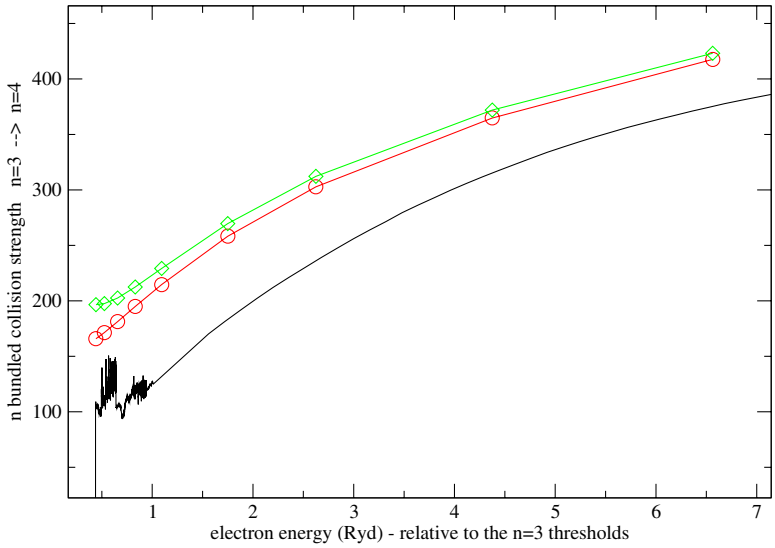


**Figure 7.** $Li^{2+}$: Bundled $n = 3$–4 collision strength. Diamonds, non-unitarized distorted wave; circles, distorted wave (Clark 1990); solid curve, present results.

### *3.5. $O^{7+}$*

Resonance-resolved hydrogenic systems that take into account the loss of electron flux into ionizing channels was systematically studied within $n = 2$ models including pseudo-states by Abu-Salbi and Callaway (1981), both for carbon and oxygen. Our experience with $C^{5+}$ shows that, when a hydrogenic target is ionized five or more times, we get diminishing returns from the inclusion of pseudo-states. Therefore, we have decided to omit them for more highly ionized cases. This not only reduces the size of the inner-region Hamiltonian which we have to diagonalize, but also reduces the scattering channels associated with the pseudo-states. This results in smoother collision strengths above the ionization limit and precludes any pseudo-resonance features. Our $n = 5$ model includes significantly more Rydberg structure compared with Abu-Salbi *et al*, due to the inclusion of $n = 3$–5 terms. They noted only a maximum difference of 6% in the case of their 1s–2*l* thermally averaged cross sections, but have started tabulating at temperatures in excess of $5.8 \times 10^5$ K where the resonance contributions are engulfed by the background collision strength. Non-dipole excitations from the ground state to $n = 4$ terms are more sensitive to resonance contributions, especially at low temperatures.

### *3.6. $Ne^{9+}$*

Consistent with the reasons outlined for the previous ion (i.e. $O^{7+}$), we did not incorporate pseudo-states into this calculation, but included an extra layer of spectroscopic terms. The inclusion of an $n = 6$ layer, especially the 6s orbital, extended the $R$-matrix hypersphere in this case by 30% further than for the $n = 5$ in $O^{7+}$. Therefore, given the promising comparison between the last three graphs of figure 4, it may be better to implement an extrapolation scheme beyond this species for high temperature effective collision strengths. However, at lower temperatures $Z^4$ scaling of increasingly ionized targets demands the highest degree of resonance resolution if we are not to introduce any errors. As with previous calculations in this isoelectronic sequence, there are no pseudo-states included in this 21 term $R$-matrix calculation so we should expect smooth collision strengths throughout.

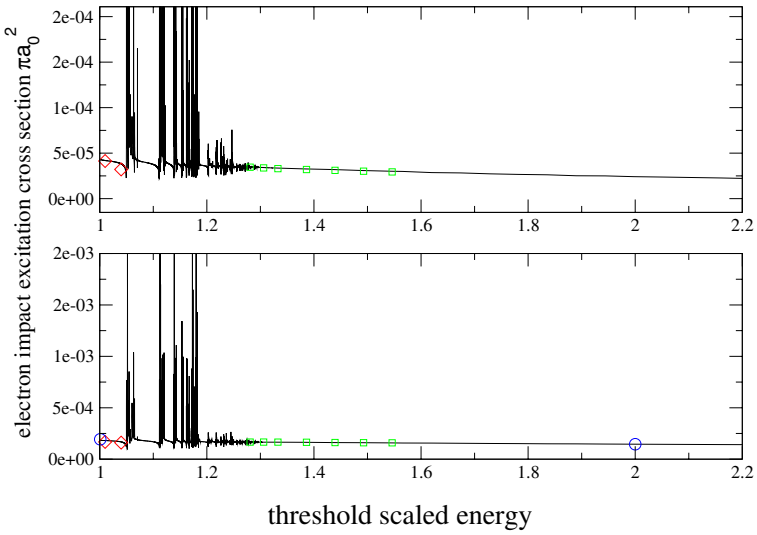


**Figure 8.** Electron-impact excitation collision strengths for $Ne^{9+}$, 1s–2s (top) and 1s–2p (bottom). The electron energy is given in threshold units. Diamonds, Morgan (1980); circles, Mitra and Sil (1978); squares, Aggarwal and Kingston (1991b); solid curve, present results.

The outer region has at most 56 scattering channels with a mesh of 10 000 energy points below the ionization threshold. Above this limit, the gradient of the dipole allowed collision strengths is not as steep as in the singly/doubly ionized cases and, hence, we have used only 25 points up to 225 Ryd.

Aggarwal and Kingston (1991b) carried out a smaller $R$-matrix calculation and their results are in good agreement with the present results (see figure 8). Further limited comparisons are made with the low-energy results of Morgan (1980) and the Coulomb–Born/CBO work of Mitra and Sil (1978) within figure 8. At a threshold scaled energy of 2, the latter results are in complete agreement with our own.

## 4. Overview and conclusion

An overview of the electron-impact excitation of light hydrogenic systems has revealed that beyond the $C^{5+}$ case, the inclusion of pseudo-states begins to have a minimal effect on Maxwell averaged collision strengths. The inclusion of equivalent high-lying bound states with $n \geqslant 7$ is now possible with recent parallel code development (Mitnik *et al* 2001). But, in the hydrogenic case, figure 3 suggests that scaled extrapolation for $n = 7$ and 8 levels could be attained to a high degree of accuracy. Figure 3 clearly shows remarkable similarity for all eight graphs and, in the case of 1s–2s, the comparison remains good for $He^+$ and $Li^{2+}$ (figure 2). Furthermore, due to our finite $R$-matrix basis and the requirements of $S$-matrix unitarity, excitations to the final layer of terms in any $R$-matrix calculations will be inflated, but as we include higher terms $n > 6$, we may have to extend this to the last two layers.

Coupling to high bound/continuum states is greatest when there is a large energy separation between the initial and final term. In hydrogenic cases these are excitations from the ground state. The proximity of the final term to the ionization limit also affects the collision strength and if we are to include more terms with higher principal quantum numbers this will only increase.

A substantial amount of effective collision strength data has been produced over a range of temperatures for $\Delta n > 0$ and $n \leqslant 5$ for $He^{+}$–$Ne^{9+}$, which should contribute to future spectroscopic modelling studies.

## Acknowledgments

In this work, CPB was supported by a US DoE SciDAC grant (DEFG02-01ER54G44) to Auburn University. We acknowledge the use of the NIFS database http://dbshino.nifs.ac.jp/ for tabulations of $Ne^{9+}$ excitation data. ESS was acting in a personal capacity, and acknowledges the use of computing equipment at NAG Ltd.

## References

Abu-Salbi N and Callaway J 1981 *Phys. Rev.* A **24** 2372–86
Aggarwal K M, Callaway J, Kingston A E and Unnikrishnan K 1992 *Astron. Astrophys. Suppl. Ser.* **80** 473–7
Aggarwal K M and Kingston A E 1991a *J. Phys. B: At. Mol. Opt. Phys.* **24** 4583–602
Aggarwal K M and Kingston A E 1991b *Phys. Scr.* **44** 517–27
Anderson H, Ballance C P, Badnell N R and Summers H P 2000 *J. Phys. B: At. Mol. Opt. Phys.* **33** 1255–62
Badnell N R 1997 *J. Phys. B: At. Mol. Opt. Phys.* **30** 1–11
Badnell N R and Gorczyca T W 1997 *J. Phys. B: At. Mol. Opt. Phys.* **30** 2011–9
Ballance C P, Badnell N R, Griffin D C, Loch S D and Mitnik D M 2002 *J. Phys. B: At. Mol. Opt. Phys.* **36** 235–46
Berrington K A and Clark R E H 1993 *Nucl. Fusion Suppl.* **3** 87–95
Berrington K A, Eissner W B and Norrington P H 1995 *Comput. Phys. Commun.* **92** 290–420
Bray I 1994 *Phys. Rev.* A **49** 1066–82
Bray I and Stelbovics A T 1993 *Phys. Rev. Lett.* **70** 746–9
Burgess A, Chidichimo M C and Tully J A 1997 *J. Phys. B: At. Mol. Opt. Phys.* **30** 33–57
Burgess A and Tully J A 1992 *Astron. Astrophys.* **254** 436–53
Burke V M, Burke P G and Scott N S 1992 *Comput. Phys. Commun.* **69** 76–98
Clark R E H 1990 *Astrophys. J.* **354** 382–6
Kisielius R, Berrington K A and Norrington P H 1996 *Astron. Astrophys. Suppl. Ser.* **118** 157–62
Mitnik D M, Griffin D C and Badnell N R 2001 *J. Phys. B: At. Mol. Opt. Phys.* **34** 4455–73
Mitnik D M, Griffin D C, Ballance C P and Badnell N R 2003 *J. Phys. B: At. Mol. Opt. Phys.* **36** 717–30
Mitra C and Sil N C 1978 *Phys. Rev.* A **18** 1758–61
Morgan L A 1980 *J. Phys. B: At. Mol. Phys.* **13** 3703–15
Norrington P H and Grant I P 1987 *J. Phys. B: At. Mol. Phys.* **20** 4869–81
Phaneuf R A, Janev J A and Pindzola M S (ed) 1987 Atomic data for fusion *Collisions of Carbon and Oxygen Ions with Electrons, H, $H_2$ and He* vol 5 ORNL-6090
Pradhan A K and Gallagher J W 1992 *At. Data Nucl. Data Tables* **52** 227–317
Summers H P 1994 *JET Joint Undertaking Report* JET-IR(94)06
Summers H P 1999 *ADAS User Manual Version 2.1* http://adas.phys.strath.ac.uk
Unnikrishnan K, Callaway J and Oza D H 1991 *Phys. Rev.* A **43** 5966–70
Whiteford A D, Badnell N R, Ballance C P, O'Mullane M G, Summers H P and Thomas A L 2001 *J. Phys. B: At. Mol. Opt. Phys.* **34** 3179–91